



# Multi-zone optimisation of high-rise buildings using artificial intelligence for sustainable metropolises. Part 2: Optimisation problems, algorithms, results, and method validation

Berk Ekici<sup>a,\*</sup>, Z. Tuğçe Kazanasmaz<sup>b</sup>, Michela Turrin<sup>a</sup>, M. Fatih Taşgetiren<sup>c</sup>, I. Sevil Sariyildiz<sup>a</sup>

<sup>a</sup> Delft University of Technology, Faculty of Architecture and the Built Environment, Chair of Design Informatics, Julianalaan 134, 2628 BL, Delft, the Netherlands

<sup>b</sup> Izmir Institute of Technology, Department of Architecture, Gulbahce Kampus, Urla, 35430, Izmir, Turkey

<sup>c</sup> Yasar University, Department of International Logistics Management, Universte Caddesi No:37-39, Agacli Yol, Bornova, 35100, Izmir, Turkey

## ARTICLE INFO

### Keywords:

Performance-based design  
Building simulation  
Sustainability  
High-rise building  
Machine learning  
Optimization

## ABSTRACT

High-rise building optimisation is becoming increasingly relevant owing to global population growth and urbanisation trends. Previous studies have demonstrated the potential of high-rise optimisation but have been focused on the use of the parameters of single floors for the entire design; thus, the differences related to the impact of the dense surroundings are not taken into consideration. Part 1 of this study presents a multi-zone optimisation (MUZO) methodology and surrogate models (SMs), which provide a swift and accurate prediction for the entire building design; hence, the SMs can be used for optimisation processes. Owing to the high number of parameters involved in the design process, the optimisation task remains challenging. This paper presents how MUZO can cope with an enormous number of parameters to optimise the entire design of high-rise buildings using three algorithms with an adaptive penalty function. Two design scenarios are considered for quad-grid and diagrid shading devices, glazing type, and building-shape parameters using the setup, and the SMs developed in part 1. The optimisation part of the MUZO methodology reported satisfactory results for spatial daylight autonomy and annual sunlight exposure by meeting the Leadership in Energy and Environmental Design standards in 19 of 20 optimisation problems. To validate the impact of the methodology, optimised designs were compared with 8748 and 5832 typical quad-grid and diagrid scenarios, respectively, using the same design parameters for all floor levels. The findings indicate that the MUZO methodology provides significant improvements in the optimisation of high-rise buildings in dense urban areas.

## 1. Introduction

The demand for high-rise buildings is increasing in metropolises owing to population growth and urbanisation trends (Ali and Al-Kodmany, 2012). For realising sustainable urban areas, sustainable high-rise buildings should be one of the topics under investigation because they consume a significant amount of energy owing to their excessively large size (Ali and Armstrong, 2008). Designing a sustainable high-rise building is a complex task because the process involves various types of design parameters that affect multiple performance aspects. Rafiei and Adeli (2016) presented robust optimisation algorithms and neural dynamic models for investigating sustainable high-rise alternatives to cope with this complexity. The previous works mentioned in part 1 showed that optimisation algorithms and machine

learning techniques have been widely used for designing sustainable high-rise buildings over the last two decades. However, in none of these studies, were the various floor levels considered as separate design problems, which is crucial for improving the overall performance of high-rise buildings (Wood, 2007). Using the same design parameters for the entire high-rise design is a limited approach because the performance of the building varies between the ground and sky floor levels in dense urban areas. Optimising the design of an entire high-rise building is challenging as the simulations require expensive computational time, and the optimisation process needs to cope with an enormous number of design parameters. The use of multi-zone optimisation (MUZO) methodology is proposed to divide high-rise buildings into subdivisions (zones) to be considered as separate problems using artificial intelligence methods to address both aspects. Part 1 of the study is focused on solving computationally expensive simulations of each zone using

\* Corresponding author.

E-mail addresses: [B.Ekici-1@tudelft.nl](mailto:B.Ekici-1@tudelft.nl) (B. Ekici), [tugcekazanasmaz@iyte.edu.tr](mailto:tugcekazanasmaz@iyte.edu.tr) (Z.T. Kazanasmaz), [M.Turrin@tudelft.nl](mailto:M.Turrin@tudelft.nl) (M. Turrin), [fatih.tasgetiren@yasar.edu.tr](mailto:fatih.tasgetiren@yasar.edu.tr) (M.F. Taşgetiren), [I.S.Sariyildiz@tudelft.nl](mailto:I.S.Sariyildiz@tudelft.nl) (I.S. Sariyildiz).

<https://doi.org/10.1016/j.solener.2021.05.082>

Received 25 October 2020; Received in revised form 9 May 2021; Accepted 26 May 2021

Available online 16 June 2021

0038-092X/© 2021 The Authors. Published by Elsevier Ltd on behalf of International Solar Energy Society. This is an open access article under the CC BY license

(<http://creativecommons.org/licenses/by/4.0/>).

Nomenclature	
<i>Daylight metrics and material properties</i>	
ASE	Annual sunlight exposure [%]
DGP	Daylight glare probability
g-val	G value of the glazing material
sDA	Spatial daylight autonomy [%]
U-val	U value of the glazing material [W/m <sup>2</sup> K]
Tvis	Visible transmittance of the glazing material
<i>Machine learning and optimisation</i>	
CMA-ES	Covariance matrix adaptation with evolution strategy
CPU	Average computation time for one replication
EC	Evolutionary computation
FES	Number of function evaluations
FES/CPU	The number of completed function evaluations in 1 s
jEDE	Self-adaptive differential evolution with an ensemble of mutation strategies
maxf(x)	Maximum of function x
NFL	No free lunch
RbfOpt	Radial basis function optimisation
SM	Surrogate model
stdf(x)	Standard deviation of function x
<i>Others</i>	
GH	Grasshopper 3D algorithmic modelling environment
IES	Illuminating Engineering Society
LEED	Leadership in Energy and Environmental Design
MUZO	Multi-zone optimisation
PCA	Performative computational architecture

surrogate models (SMs). Part 2 deals with the optimisation challenge, wherein each zone is considered as a design problem using algorithms belonging to different optimisation domains. In parts 1 and 2 of the MUZO study, quad-grid and diagrid scenarios with the shading device, glazing type, and building-shape parameters were used to demonstrate the proposed methodology.

This study is focused on optimising the entire design of high-rise buildings for quad-grid and diagrid scenarios using the 40 SMs developed in part 1. The performance aspects of the study take into consideration the two daylight metrics of Leadership in Energy and Environmental Design (LEED) v4.1., namely, the spatial daylight autonomy (sDA) and annual sunlight exposure (ASE). The optimisation process uses phase 3 of the MUZO methodology for single-objective constrained formulation with three algorithms: self-adaptive differential evolution with an ensemble of mutation strategies (jEDE) in the Optimus plug-in (Cubukcuoglu et al., 2019), radial basis function optimisation (RbfOpt), and covariance matrix adaptation with evolution strategy (CMA-ES) in the Opossum plug-in (Wortmann, 2017b). In addition, an adaptive penalty function, called the near-feasibility threshold (NFT) (Coit and Smith, 1996; Smith and Coit, 1997), is used for each optimisation algorithm in the Grasshopper 3D algorithmic modelling environment (GH) (Rutten, 2015). The paper reports the optimisation results of 20 problems for two scenarios, which comprise 260 and 220 design parameters, respectively, with the aforementioned algorithms for five replications. Part 2 of the study also validates the significance of the proposed methodology by presenting a comparison of the performances of the optimised high-rise designs and typical high-rise scenarios generated by the same design parameters for all the floor levels. The optimisation results and validation of the method show that the MUZO methodology can play a significant role in investigating sustainable high-rise alternatives in metropolises. The rest of this paper is structured as follows: Section 2 presents the state of the art for sDA and ASE optimisation, Section 3 introduces the optimisation problems and algorithms of this paper, Section 4 reports the optimisation results, Section 5 presents the validation of the MUZO methodology, Section 6 discusses the importance and potential of MUZO with surrogate-based design optimisation, and Section 7 presents the conclusions of this paper.

## 2. State of the art for sDA and ASE optimisation

This section presents the previous optimisation studies for the sDA and ASE daylight metrics of LEED within the performative computational architecture (PCA) framework in two subsections: one presenting conventional optimisation and the other computational optimisation. Conventional methods comprise an analysis of the predefined design parameters, whereas computational methods involve the use of optimisation algorithms while automating the PCA framework to investigate the best design performance. Subsequently, the novelty of this study is summarised.

### 2.1. Conventional optimisation

Over the last decade, sDA and ASE metrics have been used to investigate daylight performance and visual comfort for various building functions. An early study was focused on a classroom case with the use of three optimisation approaches while using the optical properties and size of a south-facing window (Kazanasmaz et al., 2016). Owing to the classroom requirements, the authors maximised sDA<sub>500/50%</sub> to evaluate an illuminance level of 500 lx with respect to ASE<sub>1000,250h</sub>. In the case of a hospital-patient room, in two studies, the window blinds were optimised by shaping the slats and the configuration of external sun-breakers on south-oriented windows to maximise sDA<sub>300/50%</sub> subject to ASE<sub>1000,250h</sub> (Sherif et al., 2016; Wagdy et al., 2017). In the case of office spaces, in three studies, sDA<sub>300/50%</sub> was maximised subject to an ASE<sub>1000,250h</sub> less than 10% as a preferable result, and between 10% and 20% as an acceptable limit for various design parameters, i.e., solar screens, 3D tessellation, fixed/dynamic shading devices, and surface reflectance (Fathy et al., 2017; Giostra et al., 2019; Palarino and Piderit, 2020). The general approach of these studies was to maximise sDA<sub>300/50%</sub>, with the exception of one study, owing to the educational requirements (Kazanasmaz et al., 2016). The ASE<sub>1000,250h</sub> was generally considered as less than 10% as a comfort limit, while two studies considered the results of less than 20% as acceptable solutions (Giostra et al., 2019; Palarino and Piderit, 2020). In addition, in the aforementioned studies, a limited number of design alternatives that might be related to conventional optimisation techniques were examined. Consequently, none of these studies were focused on optimising the daylight performance for the design of entire buildings, such as high-rise buildings.

2.2. Computational optimisation

Optimisation algorithms have been widely used to cope with the complexity of the design problem while investigating desirable sDA and ASE results for various building functions. An early example was focused on an office space to maximise sDA<sub>300/50%</sub> subject to an ASE<sub>1000,250h</sub> of less than 10% using a genetic algorithm (GA) in the Galapagos plug-in of GH while considering a single-objective formulation for kaleidocycle typology (Wagdy et al., 2015). In addition to daylight, Vera et al. (2017) addressed single objective constrained optimisation to minimise the total energy usage subject to an sDA<sub>300/50%</sub> greater than 50% and ASE<sub>2000,400h</sub> less than 20% for exterior fenestration systems of office spaces using particle swarm optimisation with the Hooke–Jeeves algorithm in GenOpt. Another example of combining performance aspects into one fitness function was examined by Yi et al. (2018) to maximise sDA<sub>300/50%</sub> and minimise ASE<sub>1000,250h</sub> and daylight glare probability (DGP) for auxetic structures with advanced daylight control systems in an office space using a GA in the Galapagos. As an alternative to single-objective constrained formulation, Tabadkani et al. (2018) and Mangkuto et al. (2018) maximised |sDA – ASE| subject to an sDA<sub>300/50%</sub> greater than 50% and 75%, and ASE<sub>1000,250h</sub> less than 10% for sun-responsive skin and light shelf design in office and hospital spaces using a GA in the Galapagos and Octopus plug-ins. In the case of multi-objective optimisation, Yi (2019) maximised the sDA<sub>300/50%</sub> and minimised ASE<sub>1000,250h</sub> with an aesthetic perception objective function using non-dominated sorting genetic algorithm II for a hotel building. Pilechiha et al. (2020) also considered the quality of the view from office windows in the optimisation of the sDA<sub>300/50%</sub>, ASE<sub>1000,250h</sub>, and energy

usage intensity while considering weighted summation and the HypE algorithm in the Octopus plug-in. As an alternative to multi-objective optimisation, Mangkuto et al. (2019) identified the simulation results for an office space with full factorial analysis of the internal shading devices to explore the non-dominated solutions while maximising sDA<sub>300/50%</sub> and minimising ASE<sub>1000,250h</sub> and DGP<sub>>0.21</sub> subject to an sDA greater than 55%, ASE less than 10%, and DGP less than 50%. Five of these studies comprised the consideration of a single objective, whereas others used multi-objective and weighted summation formulations. Three studies utilised static penalty functions that might limit the search ability during the optimisation process. Finally, none of the reviewed studies consisted of a comparison of the results of different optimisation algorithms using various initial populations (replications) for the entire design of the building.

2.3. Novelty of this paper

This study is focused on the optimisation of an entire high-rise building for the quad-grid and diagrid scenarios through phase 3 of the MUZO methodology, which is based on the use of multiple algorithms with replications for each optimisation task owing to the no free lunch (NFL) theorem (Wolpert and Macready, 1997). Because of the computational burden of optimising the entire design, the high-rise building is divided into 10 subdivisions (zones), which correspond to 10 design problems starting from the first zone (Z1) at the ground level until the tenth zone (Z10) at the sky level (Fig. 1). Forty SMs, and the high-rise setup, which were developed in part 1 of this study, were used to optimise the sDA and ASE metrics based on the simulation results

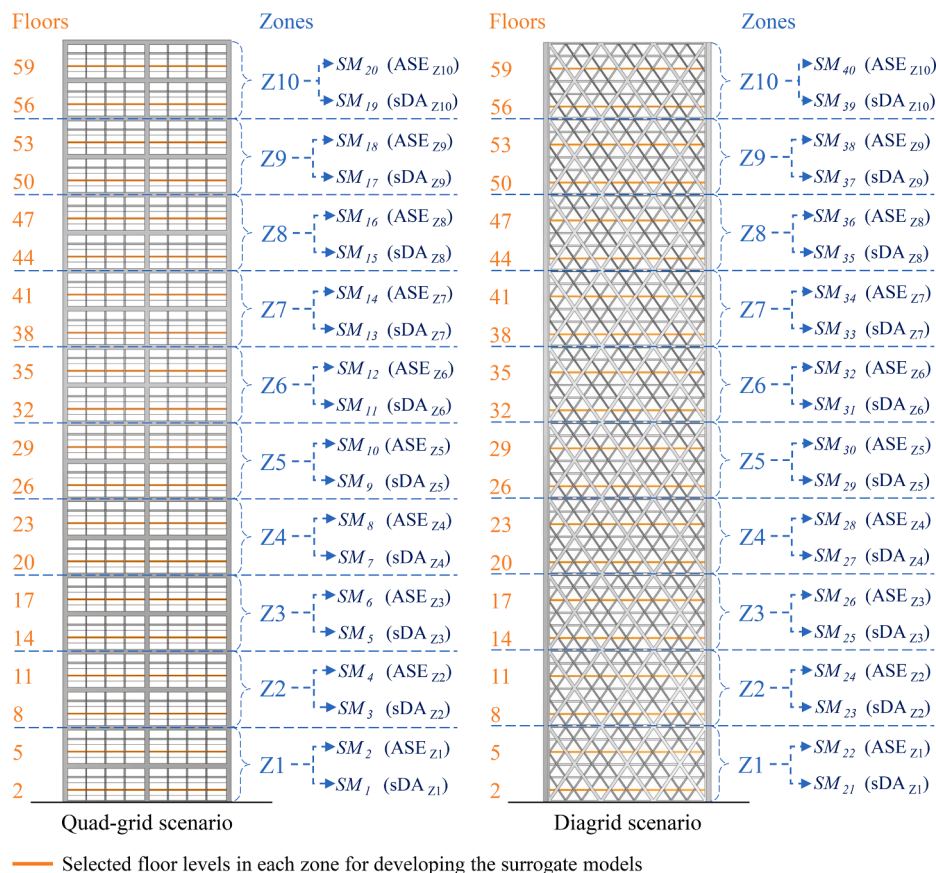


Fig. 1. Subdivisions (zones) of high-rise scenarios and their surrogate models.

obtained for the second and fifth floors in each zone. The quad-grid scenario comprises  $2.893399115e+28$  design alternatives with 26 parameters, whereas this number is  $3.054543465e+23$  for the diagrid scenario with 22 parameters in one zone. For each optimisation task, phase 3 of the MUZO methodology is considered by employing the jEDE, RbfOpt, CMA-ES algorithms, and NFT adaptive penalty function with five replications, which suggests a decision-making process using 15 optimisation results. Consequently, this paper reports on the optimised high-rise buildings after a total of 300 optimisation runs is complete, using 260 parameters for the quad-grid, and 220 parameters for diagrid, and it validates the impact of the proposed methodology by comparing the optimised scenarios with the typical high-rise scenarios. Thus, part 2 of the study not only deals with the optimisation of the entire design of high-rise buildings for the performance metrics under study, but also addresses 20 complex design problems, each having an enormous number of design alternatives in the optimisation search space, owing to the involvement of multiple design parameters.

### 3. Optimisation problems and algorithms

This section explains the problem formulation and algorithms used in each optimisation process. The first subsection explains the single-objective constrained formulation, whereas the subsequent subsections present the RbfOpt, CMA-ES, and jEDE algorithms with applications in the architecture domain. Finally, the NFT describes the adaptive penalty function for constraint handling.

#### 3.1. Problem formulation

The Illuminating Engineering Society (IES) recommends a minimum  $sDA_{300/50\%}$  of 55% with a maximum  $ASE_{1000,250h}$  of 10% as desirable daylight with acceptable comfort (IES, 2013). However, the LEED standards acknowledge design proposals with two points, i.e., while the  $sDA_{300/50\%}$  is greater than 55% and  $ASE_{1000,250h}$  is less than 10% for regularly occupied floor areas. When reaching a minimum of 75% of  $sDA_{300/50\%}$  with 10% of  $ASE_{1000,250h}$ , the design is acknowledged with three points. Considering the formulations of previous studies and the recommendation of the IES and the LEED standards, in this study, a single-objective constrained optimisation is considered for each design problem as

$$\begin{aligned} \max : & \quad sDA_{300/50\%} \quad X = (x_1, x_2, \dots, x_n) \quad \text{and } X \in S \\ \text{subject to : } & \quad ASE_{1000/250h} \leq ASE_{bound} \end{aligned} \quad (1)$$

where  $n$  is the number of design parameters in each zone for both quad-grid and diagrid scenarios,  $S$  is the entire search space of one zone, and  $ASE_{bound}$  is the maximum limit for direct sunlight. The state of the art shows that the ASE results can be related by more than 10% to the design of the shading devices. Because the sufficiency of shading devices is unexplored at the beginning of the optimisation processes, an adaptive ASE boundary is considered in each zone as

$$ASE_{bound} = \begin{cases} 10\% & \text{if } sDA_{300/50\%} \geq 55\% \\ 20\% & \text{if } sDA_{300/50\%} \leq 55\% \text{ and } ASE_{1000/250h} > 10\% \\ 30\% & \text{if } sDA_{300/50\%} \leq 55\% \text{ and } ASE_{1000/250h} > 20\% \end{cases} \quad (2)$$

where  $ASE_{bound}$  increases by 10% when the  $sDA$  result is less than 55%. This approach is considered in both quad-grid and diagrid scenarios to optimise the  $sDA$  and  $ASE$  metrics using the SMs. The optimisation task starts from Z1 and ends at Z10. After the best parameter set is determined in one zone for each algorithm, the optimisation process of the next zone is started. The parameters presented in part 1 of the MUZO study are also used herein (Appendix A). The [supplementary material](#)

presents the predictive models with learning scores of 40 SMs that were used during the optimisation process.

#### 3.2. Radial basis function optimisation

RbfOpt is a model-based algorithm used for solving computationally expensive problems and was recently presented by Costa and Nannicini (2018). For the unknown cost function, the algorithm constructs and iteratively refines an approximation model with sampled points. Compared to the existing open-source model-based algorithms available, RbfOpt provides two main contributions: an efficient method for automatic model selection using a cross-validation scheme, and an approach to exploit noisy but faster function evaluations. Opossum provides the RbfOpt algorithm to be used in architectural design optimisation as an open-source plug-in developed for GH (Wortmann, 2017b). RbfOpt in Opossum has been widely used for various design problems, i.e., daylight and glare problems (Wortmann, 2017a), optimal viewing angle in stadium design (Zargar and Alaghmandan, 2019), structural optimisation (Ilunga and Leitão, 2018), urban design (Wortmann and Natanian, 2020), and optimisation problems focused on building energy (Waibel et al., 2019). In this study, the optimisation process uses the default RbfOpt parameters while running the algorithm through Opossum v2.0.0.

#### 3.3. Covariance matrix adaptation with evolution strategy

CMA-ES is a well-known optimisation algorithm in the evolutionary computation (EC) domain proposed by (Hansen, 2006; Hansen et al., 2003; Hansen and Ostermeier, 2001). One of its most powerful features is that the search space can be increased or decreased in the next iteration based on the results of every solution. The algorithm uses this procedure for the multivariate normal distribution parameters (mean and sigma) and for the entire covariance matrix that belongs to the decision variable space. Opossum v1.7.0 provides a CMA-ES algorithm for design optimisation in the architecture domain as an open-source plug-in for GH. Recently, this algorithm has been used for various design problems, e.g., Waibel et al. (2019) optimised building energy problems while reporting promising results with a large evaluation budget, Zhang et al. (2020) focused on aerodynamic shape optimisation problems, and Fortich Mora (2020) used CMA-ES for the design problem of sustainable high-rise buildings. The optimisation process in this study comprises the use of Opossum v2.0.0, while considering the default features of the CMA-ES algorithm.

#### 3.4. Self-adaptive differential evolution with ensemble of mutation strategies

jEDE is a hybrid algorithm that belongs to the EC domain using differential evolution (Storn and Price, 1997), self-adaptive strategy (Brest et al., 2006), and an ensemble of mutation strategies (Mallipeddi et al., 2011). The purpose of the algorithm is to cope with high-dimensional problems in the domain of architectural design optimisation. The algorithm comprises a self-adaptive approach that converges to different directions with various rates of mutation and crossover operators. Moreover, with the ensemble idea, jEDE also selects the best mutation strategy for every dimension among predefined operators during the optimisation process. Therefore, the algorithm can adapt its search behaviour to different problems. The first application of jEDE, which is provided by Optimus v1.0.0 as an open-source plug-in for GH, was used for 30D CEC 2005 benchmark problems and a 70D structural design problem (Cubukcuoglu et al., 2019). The algorithm presented



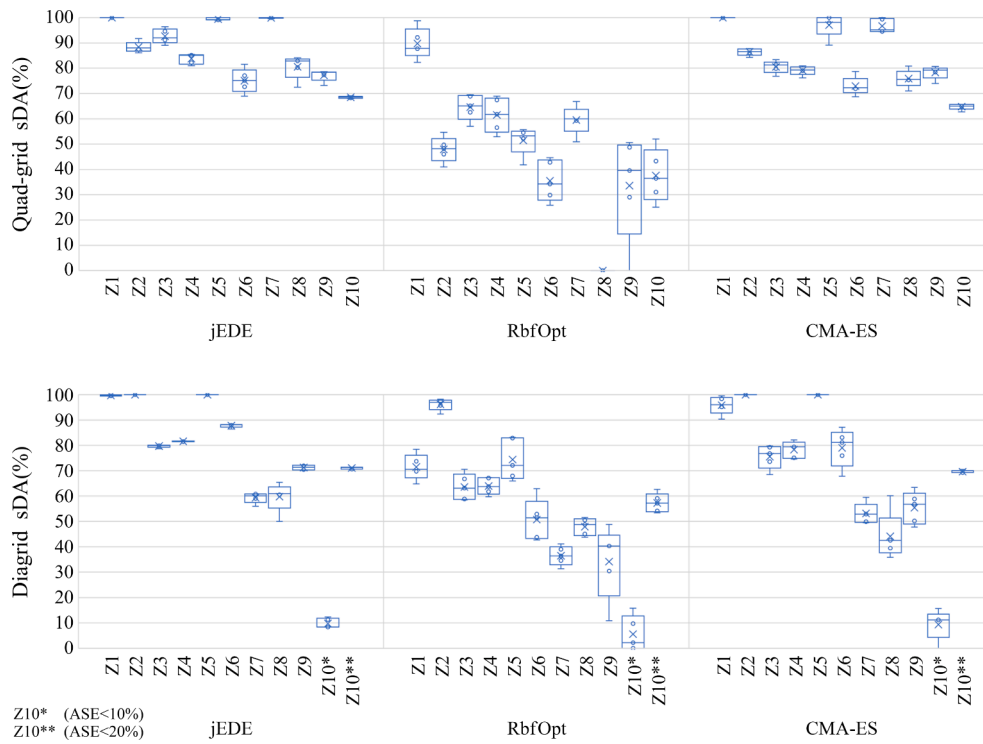


Fig. 2. Boxplots of the optimisation results.

promising results as compared with particle swarm optimisation, genetic algorithm, and RbfOpt. In addition, recent publications have demonstrated the potential of jEDE in solving a 20D problem of daylight (Ekici et al., 2019b) and the optimisation of sustainable high-rise building design focused on daylight, comfort, and energy use intensity aspects with SMs (Fortich Mora, 2020). The optimisation process in this study comprises the use of the default parameters of Optimus v1.0.2 for the jEDE algorithm.

### 3.5. Near feasibility threshold constraint handling

In previous studies mentioned in Section 2, single-objective constrained optimisation is considered as a problem formulation for the ASE and sDA metrics according to the LEED and IES standards. The general approach of these studies was to consider the ASE as a constant penalty function to be embedded in the sDA fitness function. In this method, the result of the fitness function (sDA) is multiplied with a constant value if the solution of the constraint function (ASE) is in the infeasible region. Previous studies have also discussed that the ASE results could be related to the sufficiency of the shading devices by more than 10%. Another reason for this outcome may be related to the limited search ability of the constant penalty functions. In the case of challenging constraint problems, Mallipeddi and Suganthan (2010) emphasised the importance of using advanced constraint-handling approaches. Therefore, in this study, the NFT adaptive penalty function is taken into consideration (Coit and Smith, 1996), which is an advanced version of the constant penalty function. The approach of the NFT is to define a threshold distance from a feasible region and to encourage the search within this region and the NFT neighbourhood while discouraging the search beyond that threshold. Eqs. (3) and (4) explain the penalised fitness

function  $f_p(x)$  using the NFT as

$$f_p(x) = f(x) + \left(\frac{v(x)}{NFT}\right)^\alpha \tag{3}$$

$$NFT = \frac{NFT_0}{1 + \lambda \cdot g} \tag{4}$$

where  $f(x)$  is the fitness function;  $v(x)$  is the violation;  $\alpha$  and  $\lambda$  are user-defined positive parameters taken as 2 and 0.04, respectively,  $NFT_0$  is the upper bound of the NFT taken as 0.1; and  $g$  is the generation or iteration number. The optimisation process of RbfOpt, CMA-ES, and jEDE takes into consideration the NFT approach to obtain a reasonable comparison between algorithms for each problem. The Optimus plug-in v1.0.2 provides an open-source NFT module that can work with other optimisation plug-ins in GH.

## 4. Results

The optimisation results were obtained using a computer with an Intel Xeon E5-1620 v3 core processor at 3.50 GHz, 16-GB DDR3 memory, and a 512-GB solid-state drive (Fig. 2). As the termination criterion, 10,000 was considered as the maximum number of function evaluations (FES). In the implementation of CMA-ES and RbfOpt, non-populated approaches were considered in the Opossum plug-in. Therefore, 10,000 was set as the maximum FES for CMA-ES and RbfOpt, while 40 population sizes and 250 generations were considered for the population-based jEDE algorithm. During the optimisation process, Opossum automatically stopped the iteration if there was no alteration in the fitness function. Therefore, the computation times of all the algorithms were also recorded. To evaluate the optimisation performance

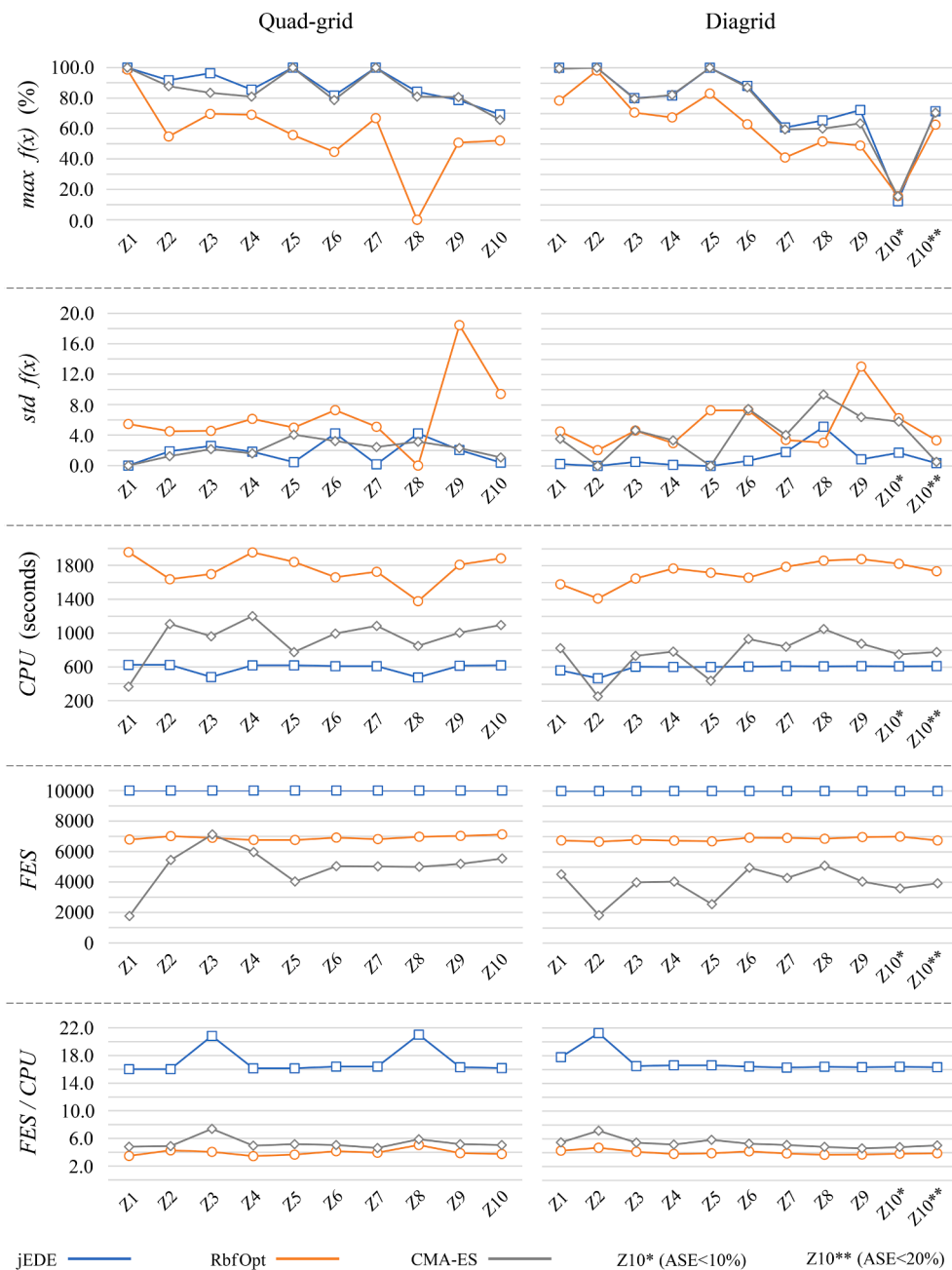


Fig. 3.  $\max f(x)$ ,  $\text{std } f(x)$ , CPU, FES, and FES/CPU for five replications.

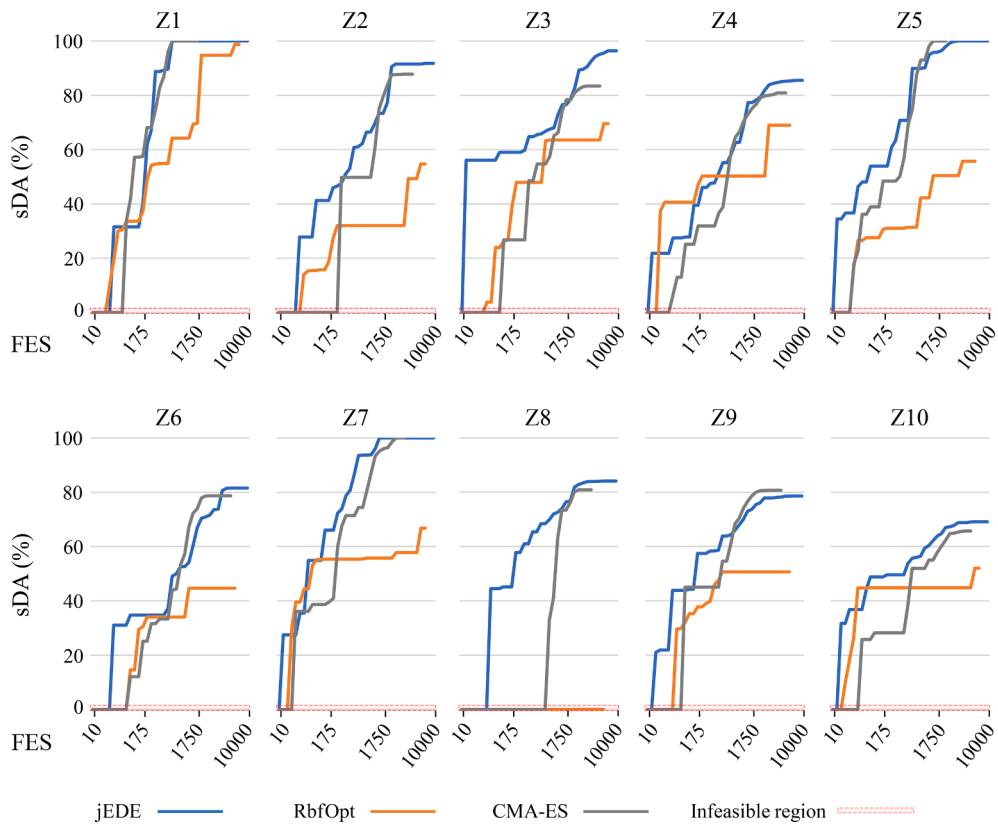


Fig. 4. Convergence graphs of the best optimisation results for the quad-grid scenario.

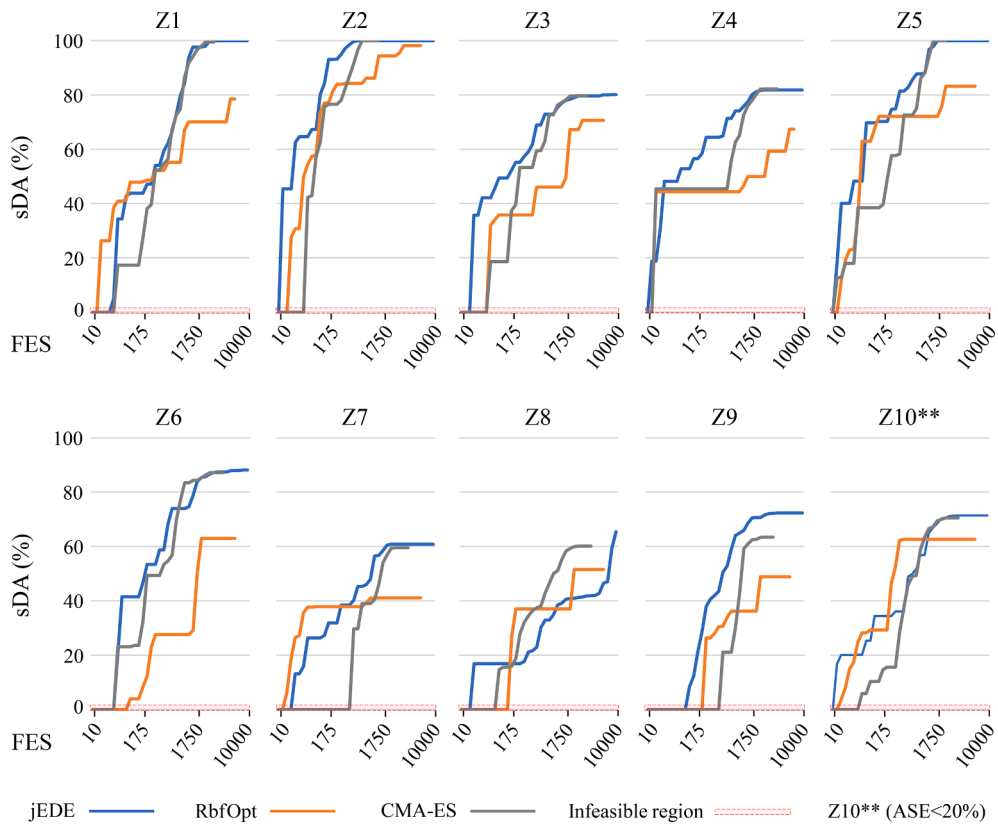


Fig. 5. Convergence graphs of the best optimisation results for the diagrid scenario.

of RbfOpt, CMA-ES, and jEDE, the following five criteria were considered:  $\max f(x)$ , and  $\text{std}f(x)$ , respectively, are the maximum, and standard deviation of the function  $x$  for five replications;  $CPU$  is the average time in seconds to complete one replication;  $FES$  is the total number of function evaluations, and  $FES/CPU$  is the number of completed function evaluations in 1 s (Fig. 3). The convergence graphs for the best results among the five replications of each algorithm are presented in Figs. 4 and 5. In addition, Appendix B presents the convergence graphs of all the replications.

In the quad-grid results, jEDE outperformed the other algorithms in six zones, whereas jEDE and CMA-ES yielded the same results in three zones, and CMA-ES outperformed jEDE in one zone. In the case of the LEED scores, jEDE and CMA-ES reached three points in nine zones, while both algorithms reached two points only in Z10. In contrast, RbfOpt reported three points for Z1, two points for Z3, Z4, Z5, and Z7, and sDA results less than 55% in other zones. Hence, the jEDE and CMA-ES could cope with the quad-grid scenario and provided satisfactory results for LEED standards, while the RbfOpt could not achieve the same result owing to the insufficient sDA levels reported for Z2, Z6, Z8, Z9, and Z10. In the diagrid results, the constraint of  $ASE_{bound} \leq 10$  resulted in undesirable sDA solutions in Z10 for all the algorithms. Thus, the boundary was increased by 10% to consider the new constraint function as  $ASE_{bound} \leq 20$ . As a result, the jEDE outperformed the other algorithms in seven zones. In two zones, jEDE and CMA-ES yielded the same results, whereas only in one zone, the CMA-ES outperformed the jEDE. In the case of the LEED scores, the jEDE and CMA-ES presented three points in six zones and two points in three zones, whereas the RbfOpt found three points in three zones, two points in three zones, and insufficient results in four zones. Therefore, the jEDE and CMA-ES could cope with the diagrid scenario, while providing satisfactory results for the LEED standards in nine zones and acceptable results ( $ASE_{bound} \leq 20$ ) in Z10, while the RbfOpt could not present a desirable performance for the entire building owing to the insufficient sDA results reported for Z7, Z8, Z9, and Z10. With respect to the computation time, the RbfOpt and CMA-ES were automatically terminated at a smaller  $FES$  than the jEDE. Based on the  $CPU$  results, the CMA-ES converged faster than the other algorithms in Z1 of the quad-grid, and Z2 and Z5 of the diagrid scenarios. In all the other problems, the jEDE converged faster than the CMA-ES and RbfOpt with less deviation in computation time despite the higher  $FES$ . In contrast, the  $FES/CPU$  results suggested that the jEDE could evaluate a single function much faster than the other algorithms.

In the optimised solutions, the results showed that the sDA values diversified in all zones for the both scenarios. For instance, optimised solutions of the lower zones presented a high percentage of sDA because the dense areas in the built environment significantly blocked direct sunlight. Thus, the daylight was controlled using shading devices and considering high-transmittance glazing materials between Z1 and Z3. In the middle zones, it was observed that the sDA values started to vary between Z4 and Z7 owing to the different shading densities and glazing types used. In the higher zones (Z8–Z10), the sDA results were lower than those in the other zones because direct sunlight met with the corresponding floors from all directions (north, south, east, and west). Therefore, either dense use of shading devices or low-transmittance glazing materials were selected, especially in the south and east orientations, to cope with this challenge. In addition, it was observed that a significant building twist would be desirable in the zones between Z8 to Z10 to decrease the impact of direct sunlight as compared with the other zones. The described design differences in the various zones were based

**Table 1**

sDA performance of the entire high-rise building design for quad-grid and diagrid scenarios.

Algorithm	Quad-grid	Diagrid
jEDE	88.7	82.0
RbfOpt	56.2	66.5
CMA-ES	85.8	80.2

on several reasons. Firstly, the density of the surroundings caused various design challenges, i.e., high building density at the ground levels and low density at the sky levels. Therefore, the optimisation algorithms found different design parameters owing to the different surrounding conditions. Secondly, higher zones were dependent on the lower zones because of the rotation and floor-to-floor height parameters. The optimised parameters in the lower zones could negatively affect the higher zones. Nevertheless, desirable solutions were obtained from the results reported after the MUZO optimisation process because the independent rotation and floor-to-floor height parameters could control the performance of each zone.

With a focus on the overall building performance based on the average results of all the zones, Table 1 presents the sDA results for the entire high-rise building. The overall results of the algorithms demonstrated that the jEDE and CMA-ES found a higher sDA in the quad-grid than in the diagrid. However, the RbfOpt presented a superior sDA performance in the diagrid scenario. Consequently, the jEDE presented the best sDA performance, while the CMA-ES presented the second-best performance, and the RbfOpt presented the third best design options. Moreover, based on the results in Figs. 2–5, we can also conclude that the quad-grid shading devices provided better daylight performance within acceptable comfort conditions as compared with the diagrid devices. Fig. 6 presents the best parameters reported after the optimisation process for both scenarios, whereas Figs. 7 and 8 illustrate these parameters in the form of high-rise buildings. The supplementary material presents the results of the optimised building designs.

## 5. Validation of the method

The design of high-rise buildings has changed owing to technological improvements, design concerns with environmental impacts, and regulation changes over time (Oldfield et al., 2009). Few buildings appear to be examples of such design concerns in the 21st century, as they comprise various building shapes and façade configurations and a combination of transparent and opaque surfaces. However, the design of high-rises using various design parameters could provide solutions for realising better building performance in dense urban districts, as discussed in this paper. This section presents the potential performance improvement that can be realised in sustainable high-rise buildings in metropolises by comparing the optimised scenarios obtained using the MUZO methodology with typical high-rise scenarios. In the majority of the existing high-rise buildings, the same parameter values are applied to the entire high-rise design (e.g., singular floor-to-floor height, same façade configuration, and a single glazing type). For profound comparisons, various combinations of parameters are defined to develop typical scenarios using the same parameters in the optimisation process. In total, 8748 typical quad-grid and 5832 typical diagrid scenarios were



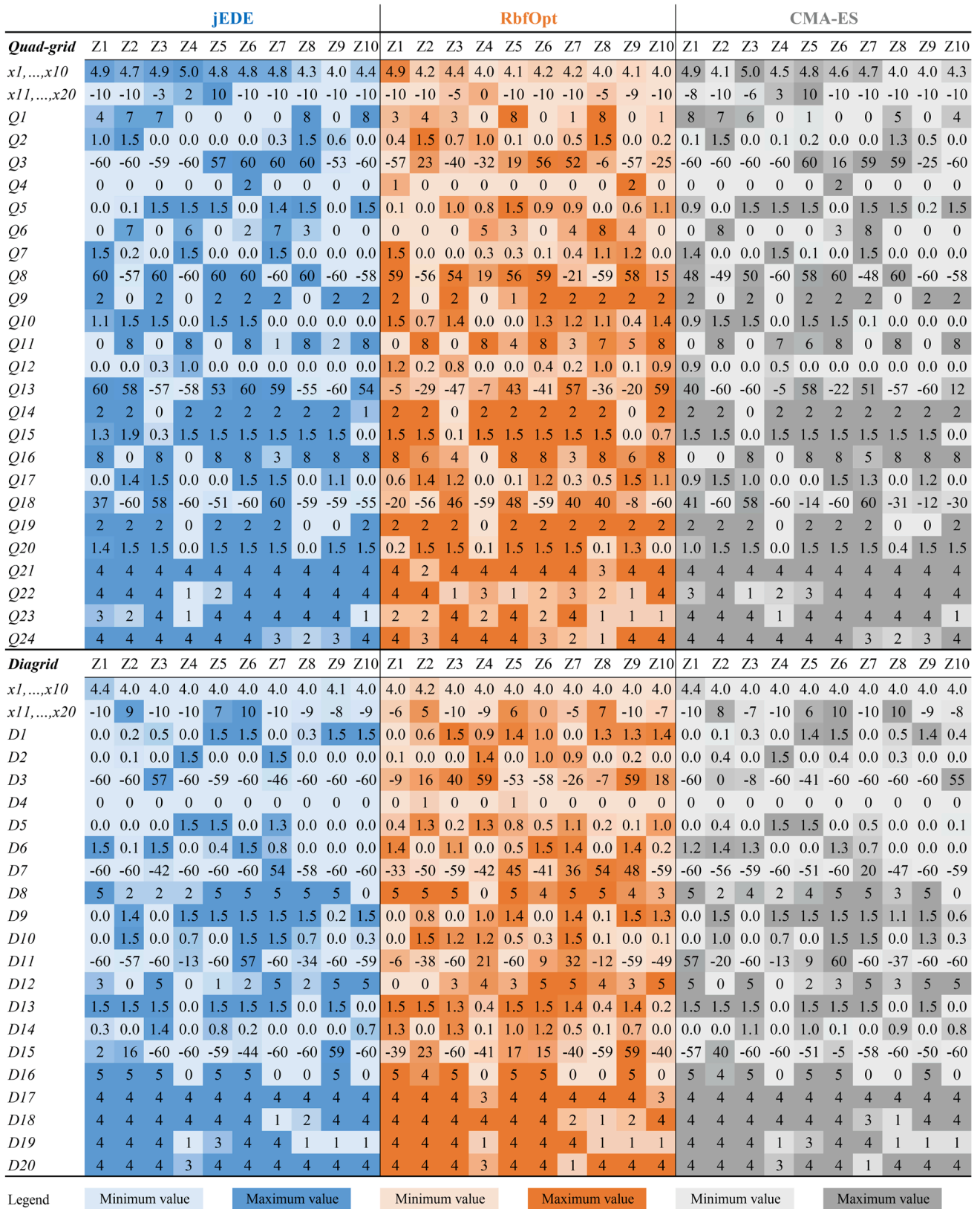


Fig. 6. Parameter maps of the optimised building designs.

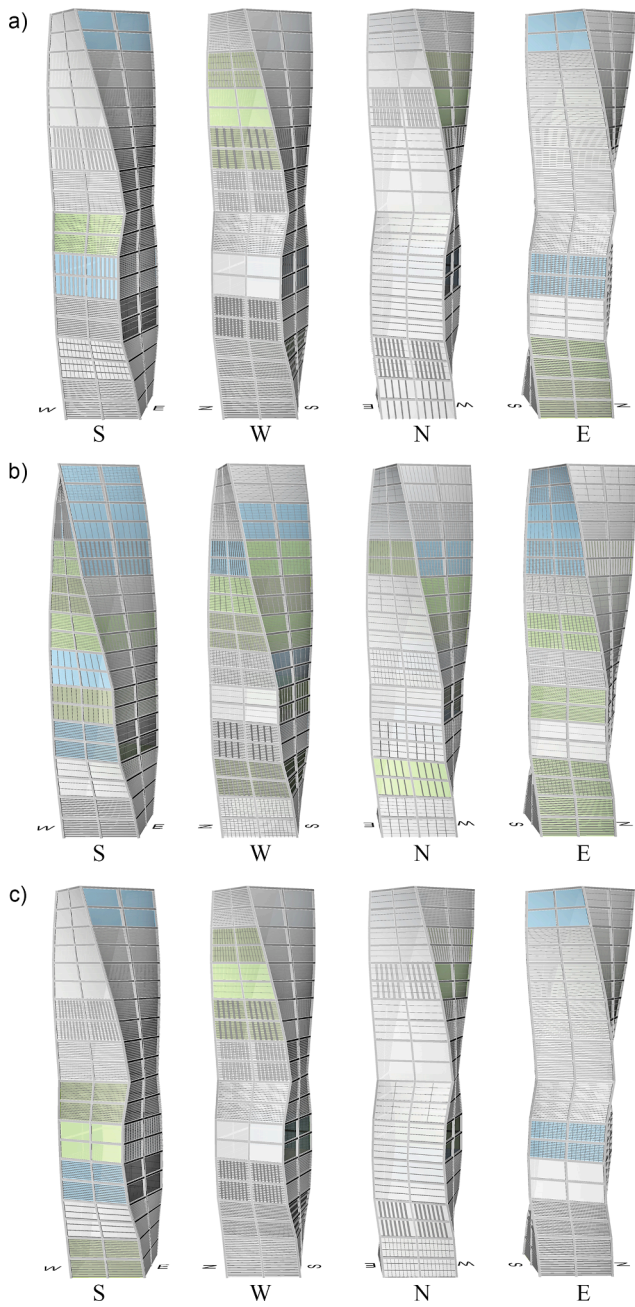


Fig. 7. jEDE (a), RbfOpt (b), and CMA-ES (c) optimised designs for the quad-grid scenario.

generated using the values listed in Table 2, and Figs. 9 and 10 illustrate several examples of these scenarios.

The performance of each typical scenario was calculated for every zone using the same SMs in a short time. The average performance results obtained for all the zones were considered to evaluate the overall building performance for the typical scenarios. In the case of the optimised scenarios, the jEDE results were used for comparison, as they were

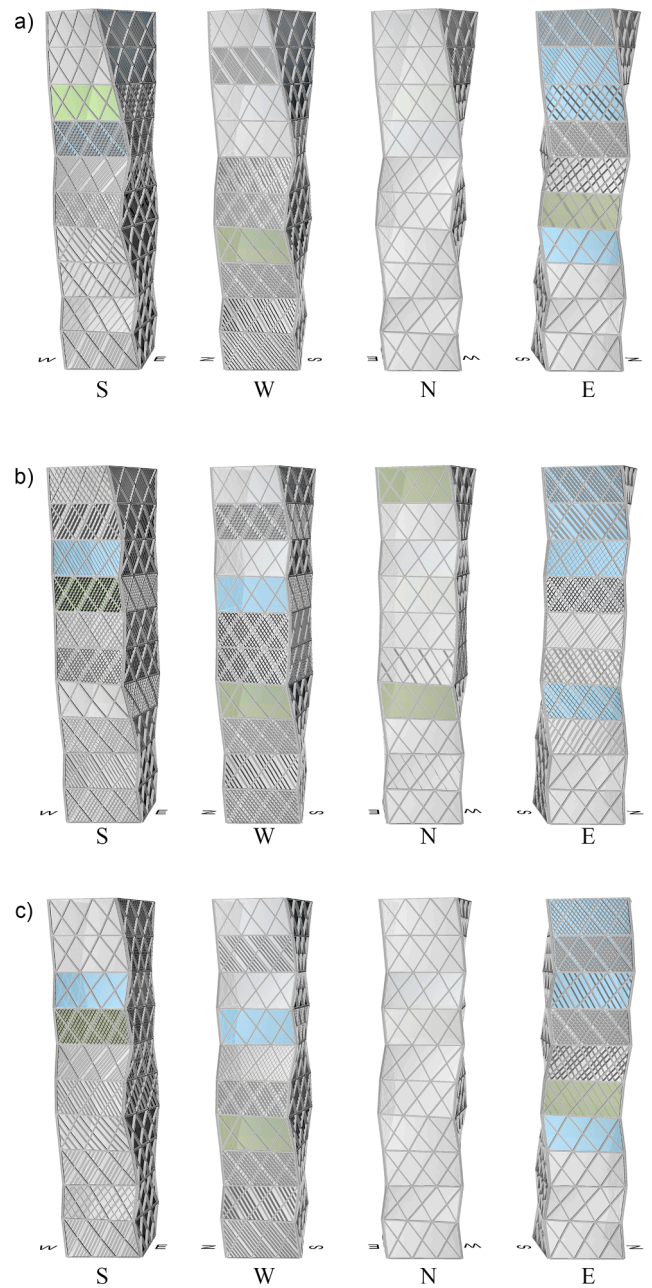


Fig. 8. jEDE (a), RbfOpt (b), and CMA-ES (c) optimised designs for the diagrid scenario.

the best proposed design solutions. Figs. 11 and 12 present comparisons of the quad-grid and diagrid scenarios, respectively. As a result, the MUZO designs exhibited the best performances with an ASE of 9.8% and sDA of 88.7% in the quad-grid scenario and an ASE of 10.5% and sDA of 82.0% in the diagrid scenario. As mentioned in the results section, owing to the insufficient shading performance of diagrid Z10,  $ASE_{bound} \leq 20$  was considered, which resulted in a slightly higher ASE performance than



**Table 2**  
Parameter values used for generating typical scenarios.

Scenario	Floor-to-floor height of zones	Rotation of zones	Number of the shading devices		Length of the shading devices			Rotation of shading devices	Glazing type	Generated scenarios
			Horizontals	Verticals	Horizontals	Verticals	1st order diagonals			
<i>Quad-grid façade</i>	[4, 4.5, 5]	[0, 4, 8]	[0, 1, 2]	[0, 4, 8]	[0.0, 0.8, 1.5]	[0.0, 0.8, 1.5]	–	[–30, 0, 30]	[1, 2, 3, 4]	8748
<i>Diagrid façade</i>	[4, 4.5, 5]	[0, 4, 8]	–	–	–	–	[0.0, 0.8, 1.5]	[–30, 0, 30]	[1, 2, 3, 4]	5832

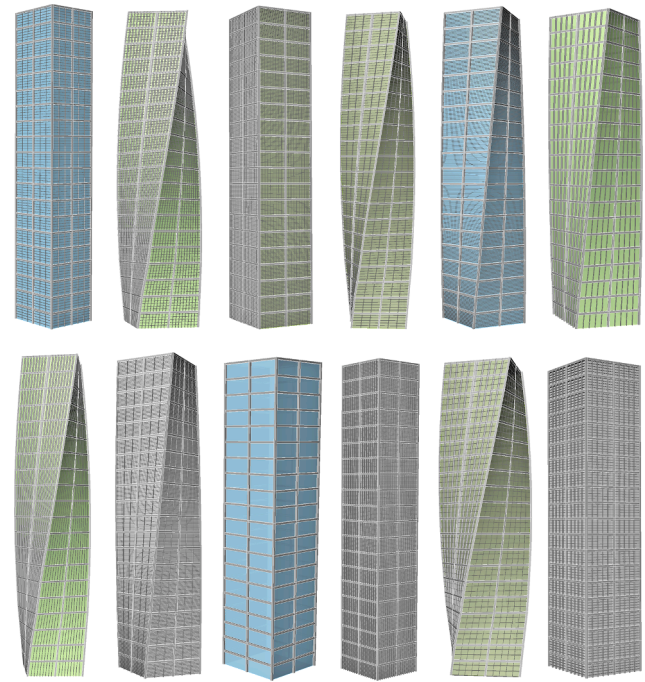


**Fig. 9.** Typical quad-grid high-rise examples.

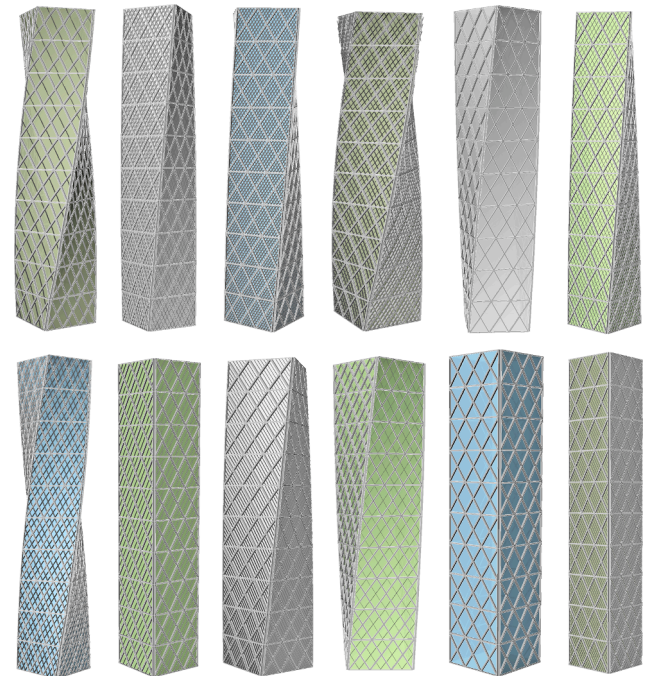


**Fig. 10.** Typical diagrid high-rise examples.

10%. Ultimately, the overall performances of the typical high-rise scenarios could not provide satisfactory LEED scores, which demonstrates the importance of using the MUZO methodology in dense urban districts.

## 6. Discussion

This section presents the discussion based on the optimisation results and the validation of the method explained in the previous sections. Firstly, two discussion topics are addressed: the importance of the MUZO methodology for metropolises, and its potential. Secondly, the ongoing

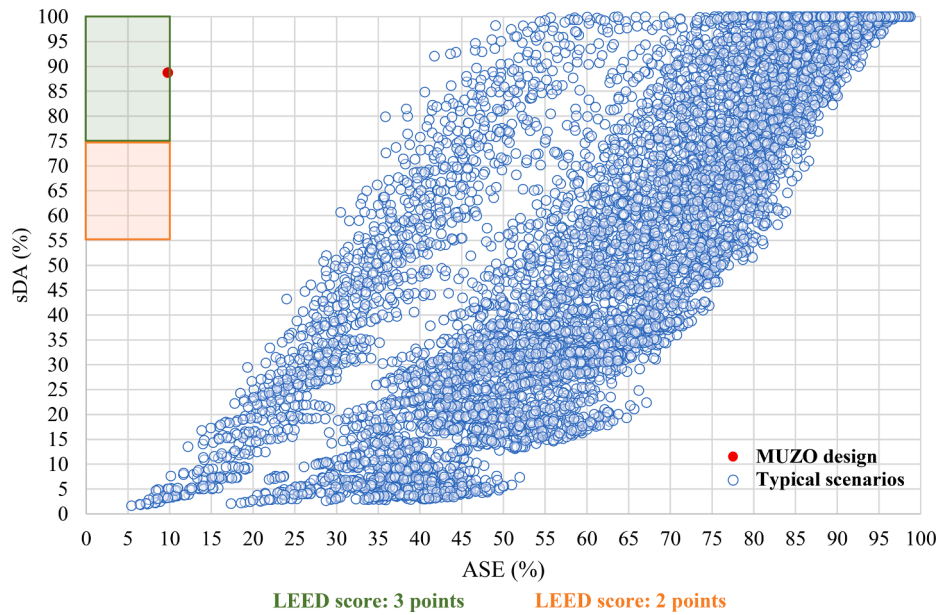


Fig. 11. Validation for quad-grid scenario (MUZO design versus 8748 scenarios).

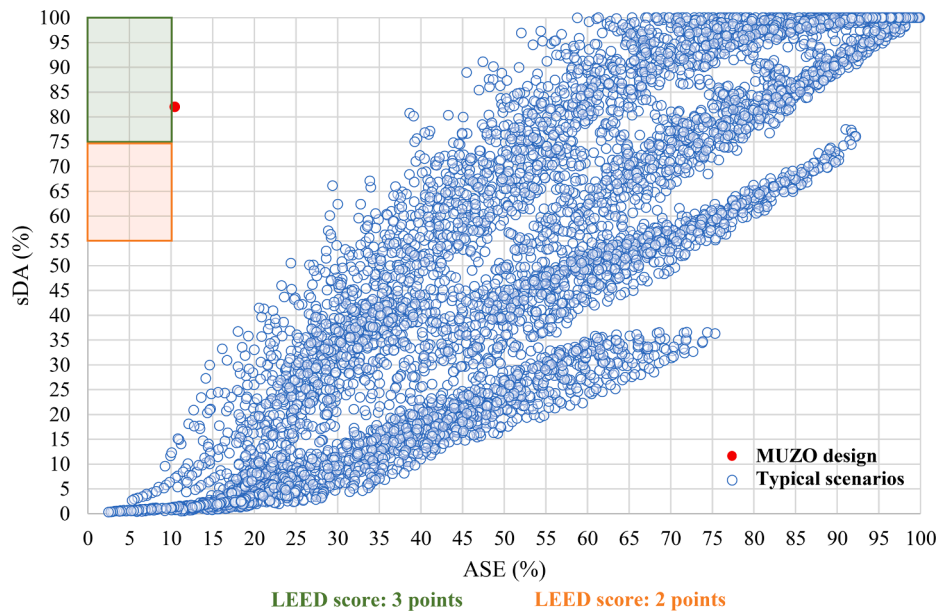


Fig. 12. Validation for diagrid scenario (MUZO design versus 5832 scenarios).

discussion in architectural design optimisation based on surrogate-based algorithms versus optimisation with SMS is focused upon.

- (1) *The importance of the MUZO methodology for future metropolises:* The results obtained in this study indicated that the MUZO methodology could present desirable performance outcomes for 20 complex design problems while considering multiple parameters related to the architecture of high-rise buildings. Recent reviews have shown that not only performance aspects related to sustainable buildings but also parameters related to architectural design may present additional complexity during the optimisation process (Attia et al., 2013; Ekici et al., 2019a; Evins, 2013; Touloupaki and Theodosiou, 2017). Therefore, the use of the MUZO methodology may support architects and engineers as they investigate sustainable high-rise scenarios by taking into consideration parameters related to design concerns in the

conceptual phase. The results also proved that the performance outcomes on different floor levels of high-rise buildings may be affected in dense urban areas. The main reason for the superior results obtained in the optimised designs proposed by the MUZO methodology was the division of one large design problem into sub-problems (zones). Hence, the optimisation algorithms could determine the best design alternatives for each zone while considering the performances of the various floor levels.

- (2) *Potential of the MUZO methodology:* This study focused on optimising the sDA and ASE daylight metrics of LEED standard to evaluate the sustainability score of high-rise buildings. The MUZO methodology may integrate more performance aspects related to sustainable buildings (e.g., energy consumption, building integrated photovoltaics, and adaptive comfort). In such a case, the formulation of the problem could comprise multi-objective or many-objective optimisation to handle more than



two conflicting performance aspects. In addition, the complexity of the problem can be controlled by varying the number of zones. In this study, ten zones were considered, which is a predefined parameter that can be changed by the decision-maker based on the density of the surroundings. The consideration of fewer zones would limit the number of design decisions for the entire high-rise design, while the use of a larger number of zones may increase the complexity and computational burden exponentially. During the optimisation process, 1,095,395 and 1,139,785 FES were considered for the quad-grid and diagrid scenarios, respectively, in order to determine which presents the best performance, and 14,580 FES were considered to evaluate the performance generated in typical high-rise scenarios. If these tasks were based on simulations, which required 4 min to calculate the performance of one design, 17.12 years would be required to complete all these computations. The MUZO methodology provided near-optimal alternatives for 4 days using SMs. Moreover, the aforementioned optimisation tasks were completed in GH using the Optimus and Opossum plug-ins. The flexibility of the proposed methodology allows the use of other digital platforms for optimisation, e.g., Python, C++, and C#, because the predictive models can be defined in another software.

(3) *Surrogate-based optimisation algorithms* versus *optimisation with SMs*: An ongoing discussion in the literature is focused on the use of either surrogate-based optimisation (e.g., RbfOpt) or SMs with heuristic optimisation algorithms (e.g., this study). While the user can optimise the design task using surrogate-based algorithms when considering a small amount of FES, the overall process still requires a significant amount of time owing to the replication of the optimisation process using simulations. However, decision-makers can investigate the design problem extensively in a reasonable amount of time using SMs, various algorithms, and replications, but with a prediction error. The accuracy of the SMs can be improved for each design problem, as explained in part 1 of this study; however, achieving zero error is almost impossible. Therefore, we can conclude that surrogate-based optimisation is convenient for small-scale design problems (e.g., office spaces), whereas optimisation with SMs is useful for large-scale design problems (e.g., high-rise buildings).

7. Conclusion

This paper presents the second part of the MUZO study and is focused on the optimisation problems and algorithms, results, and validation of the method. The results of this study showed that the performance of the entire high-rise building in dense urban districts can be improved by focusing on each zone as a separate design problem, and the optimisation process is explained in this paper. The combination of these approaches with the SMs presented in part 1 allowed us to complete the optimisations of entire high-rise buildings in a short time. The obtained results indicated satisfactory sDA and ASE performances that met the

LEED criteria in 19 out of 20 design problems comprising various complexities. Although the jEDE slightly outperformed the CMA-ES algorithm, the RbfOpt presented a lower sDA performance as compared to the other algorithms. This underscores the importance of employing various optimisation algorithms with replications in architectural design optimisation because "the global optimal of each design problem is unexplored". In addition, the validation of the method also demonstrated that the building performance achieved using the MUZO methodology exhibited a remarkable improvement as compared to that of typical high-rise scenarios in dense urban districts. Therefore, the consideration of different parameters for various floor levels may provide significant performance improvements in the design of sustainable high-rise buildings in metropolises.

In conclusion, the relevance of this study is confirmed by the obtained optimisation results and the validation of the presented method. Thus, this study underscores the affect of the use of the MUZO approach for metropolises while dividing high-rise buildings into zones to be considered as separate design problems. The importance of artificial intelligence methods for swift optimisation for determining sustainable high-rise alternatives with the use of a large number of parameters was also demonstrated. In real-world applications, there is a possibility of combining 10 zones into one objective function instead of dealing with 10 separate problems. However, the design process may involve a large number of parameters, such as 260 parameters in the quad-grid and 220 parameters in the diagrid scenarios of this study. Therefore, the domain of architectural design optimisation requires tools and algorithms that can simultaneously cope with more than 200 parameters for high-dimensional constrained problems (Chu et al., 2011; Jia et al., 2011). A sensitivity analysis could decrease the total number of design parameters; however, the final design may not reflect all the architectural concerns owing to some variables having been discarded. Another alternative to decrease the overall complexity of the design process could be the consideration of two algorithms that belong to different optimisation domains (e.g., surrogate-based and EC). Finally, in real-world applications, fewer zones may be considered, which would also decrease the computational complexity, based on the density of the urban plot under study.

Declaration of Competing Interest

The authors declare that they have no known competing financial interests or personal relationships that could have appeared to influence the work reported in this paper.

Acknowledgments

We thank our colleague Cemre Çubukçuoğlu (PhD candidate in the Chair of Design Informatics) for the collaborative work while developing the OPTIMUS plug-in for the Grasshopper 3D algorithmic modelling environment.

Appendix A. Parameters of the quad-grid and diagrid scenarios

	Parameters	Explanation	Location	Type	Unit	Boundary
<i>Quad-grid façade</i>	$x_{Q1}, x_{Q6}, x_{Q11}, x_{Q16}$	Number of vertical devices	N-S-E-W	Discrete	–	[0, 8]
	$x_{Q2}, x_{Q7}, x_{Q12}, x_{Q17}$	Length of vertical devices		Continues	m	[0.0, 1.5]
	$x_{Q3}, x_{Q8}, x_{Q13}, x_{Q18}$	Rotation of vertical devices		Discrete	°	[-60, 60]
	$x_{Q4}, x_{Q9}, x_{Q14}, x_{Q19}$	Number of horizontal devices		Discrete	–	[0, 2]
	$x_{Q5}, x_{Q10}, x_{Q15}, x_{Q20}$	Length of horizontal devices		Continues	m	[0.0, 1.5]
	$x_{Q21}, x_{Q22}, x_{Q23}, x_{Q24}$	Glazing type		Discrete	–	[1, 4]
	<i>Diagrid façade</i>	$x_{D1}, x_{D5}, x_{D9}, x_{D13}$	Length of 1st order diagonal	N-S-E-W	Continues	m
$x_{D2}, x_{D6}, x_{D10}, x_{D14}$		Length of 2nd order diagonal		Continues	m	[0.0, 1.5]

(continued on next page)

(continued)

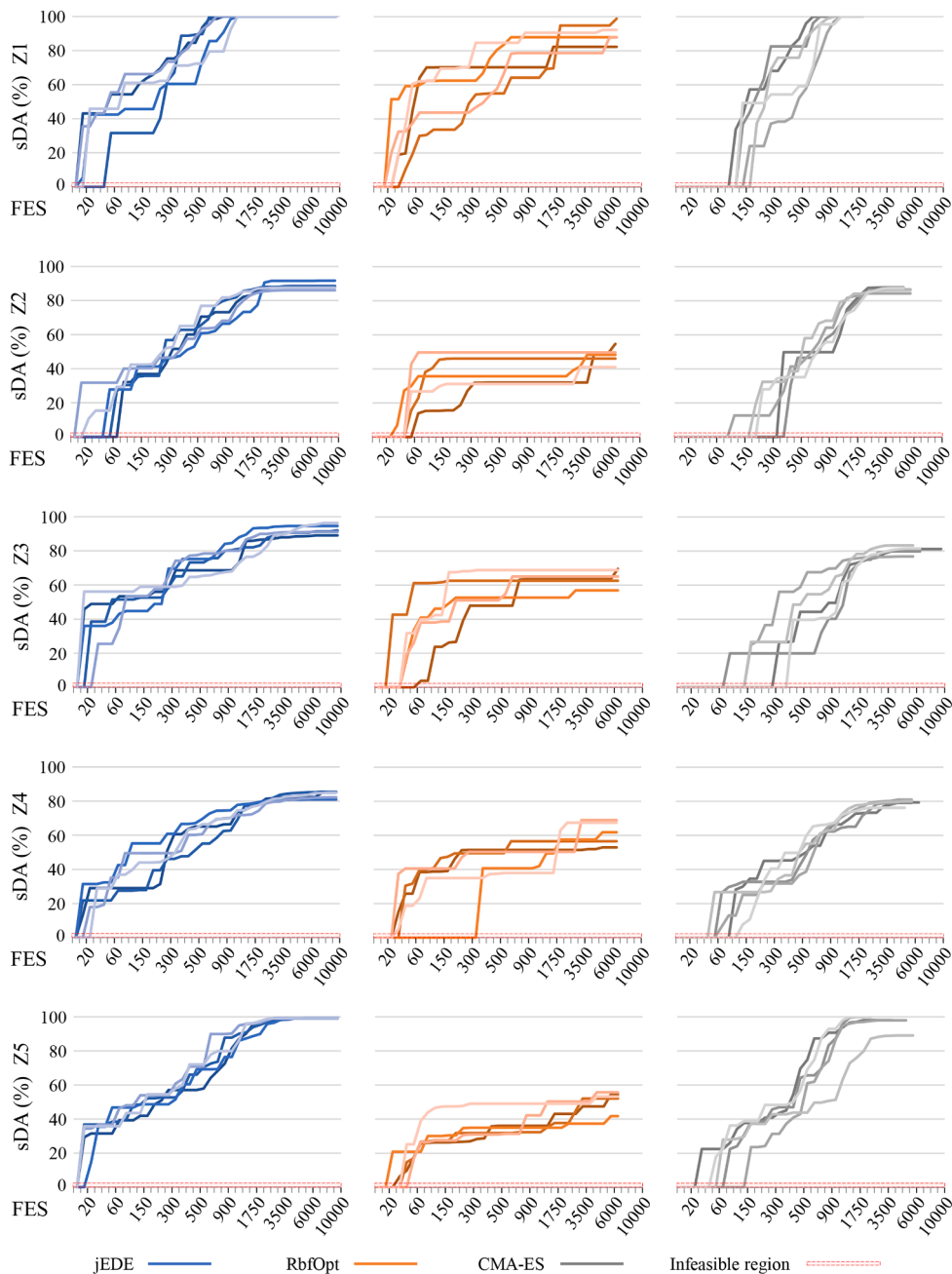
	Parameters	Explanation	Location	Type	Unit	Boundary
	$x_{D3}, x_{D7}, x_{D11}, x_{D15}$	Rotation of diagonal devices		Discrete	°	[-60, 60]
	$x_{D4}, x_{D8}, x_{D12}, x_{D16}$	Number of diagonal devices		Discrete	–	[0, 5]
	$x_{D17}, x_{D18}, x_{D19}, x_{D20}$	Glazing type		Discrete	–	[1, 4]
Building shape	$x_1, \dots, x_{10}$	Floor-to-floor height of zones	–	Continues	m	[4.0, 5.0]
	$x_{11}, \dots, x_{20}$	Rotation of zones		Discrete	°	[-10, 10]

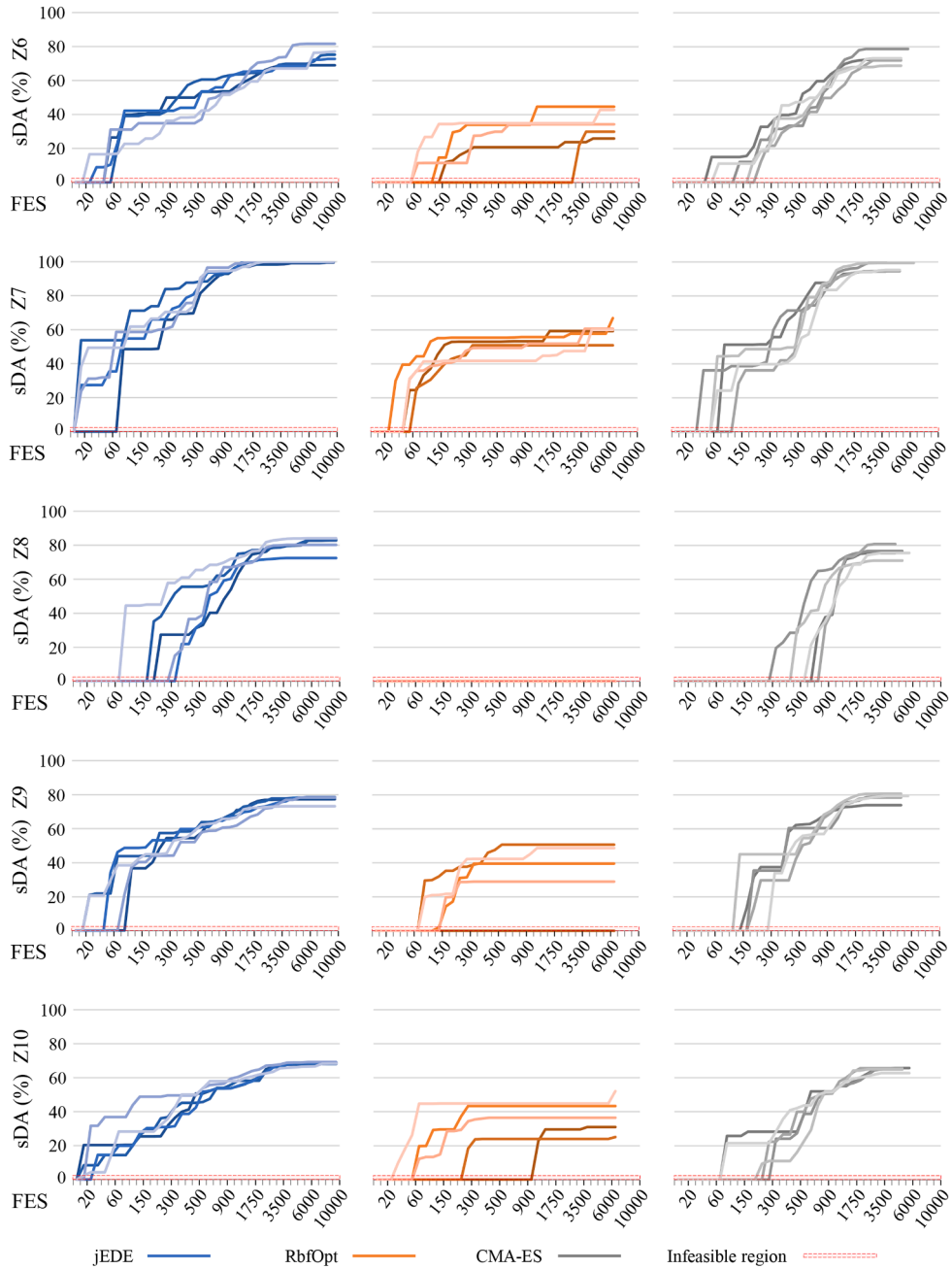
Type	Explanation	Tvis	U-val.	g-val.
Glazing types	1 Tinted float 8 mm blue – 12 mm air – Temperable Low-E 8 mm blue	0.22	1.6	0.28
	2 Temperable Low-E 8 mm neutral – 12 mm air – Clear float 8 mm – 12 mm air – Temperable Low-E 8 mm green	0.45	0.9	0.40
	3 Tinted float 8 mm green	0.68	5.6	0.51
	4 Ultra-clear float 8 mm – 12 mm air – Ultra clear float 8 mm	0.82	2.8	0.81

Appendix B

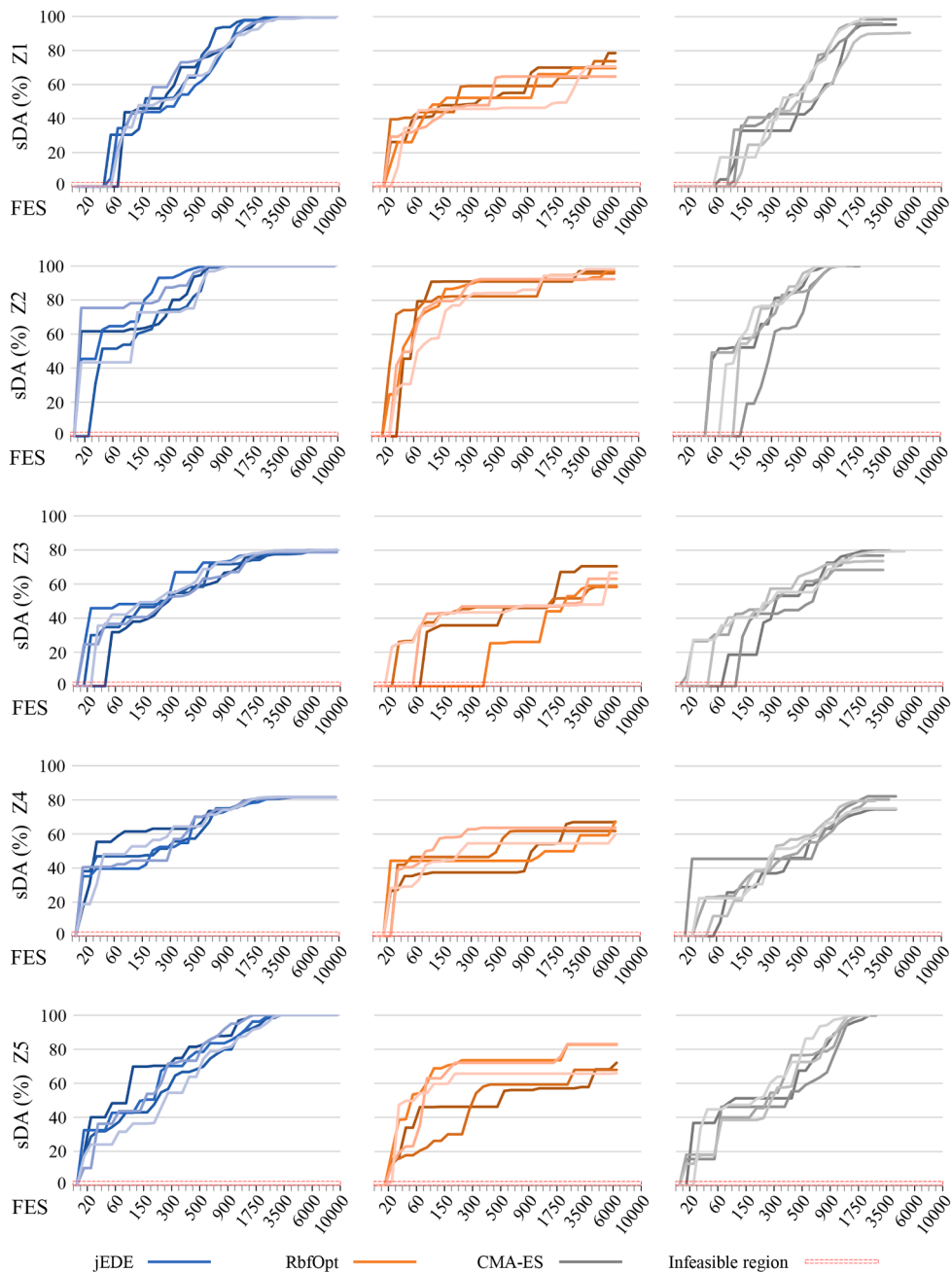
Appendix B1. Quad-grid convergence graphs for all replications from Z1 to Z5



Appendix B2. Quad-grid convergence graphs for all replications from Z6 to Z10

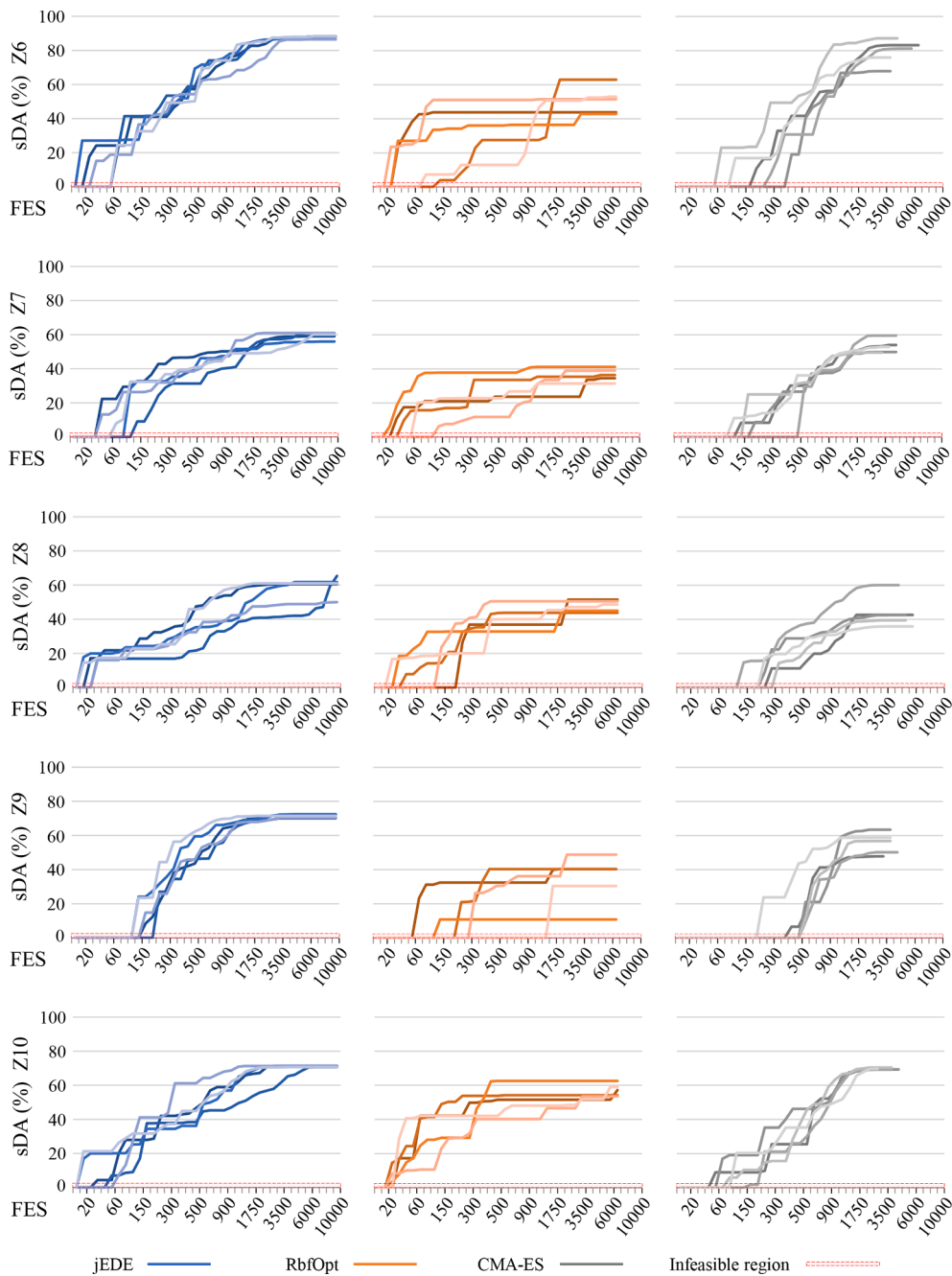


Appendix B3. Diagrid convergence graphs for all replications from Z1 to Z5





Appendix B4. Diagrid convergence graphs for all replications from Z6 to Z10



Appendix C. Supplementary material

Supplementary data to this article can be found online at <https://doi.org/10.1016/j.solener.2021.05.082>.

References

Ali, M.M., Al-Kodmany, K., 2012. Tall buildings and urban habitat of the 21st century: a global perspective. *Buildings* 2 (4), 384–423.  
 Ali, M.M., Armstrong, P.J., 2008. Overview of sustainable design factors in high-rise buildings. In: *Proc. of the CTBUH 8th World Congress*, pp. 3–5.

Attia, S., Hamdy, M., O'Brien, W., Carlucci, S., 2013. Assessing gaps and needs for integrating building performance optimization tools in net zero energy buildings design. *Energy Build.* 60, 110–124.  
 Brest, J., Greiner, S., Boskovic, B., Mernik, M., Zumer, V., 2006. Self-adapting control parameters in differential evolution: A comparative study on numerical benchmark problems. *IEEE Trans. Evol. Comput.* 10 (6), 646–657.  
 Chu, W., Gao, X., Sorooshian, S., 2011. A new evolutionary search strategy for global optimization of high-dimensional problems. *Inf. Sci.* 181 (22), 4909–4927.

- Coit, D.W., Smith, A.E., 1996. Penalty guided genetic search for reliability design optimization. *Comput. Ind. Eng.* 30 (4), 895–904.
- Costa, A., Nannicini, G., 2018. RBFOpt: an open-source library for black-box optimization with costly function evaluations. *Math. Programm. Comput.* 10 (4), 597–629.
- Cubukcuoglu, C., Ekici, B., Tasgetiren, M.F., Sariyildiz, S., 2019. OPTIMUS: Self-Adaptive Differential Evolution with Ensemble of Mutation Strategies for Grasshopper Algorithmic Modeling. *Algorithms* 12 (7), 141.
- Ekici, B., Cubukcuoglu, C., Turrin, M., Sariyildiz, I.S., 2019a. Performative computational architecture using swarm and evolutionary optimisation: A Review. *Build. Environ.* 147, 356–371.
- Ekici, B., Kazanasmaz, T., Turrin, M., Tasgetiren, M.F., Sariyildiz, I.S., 2019b. A Methodology for daylight optimisation of high-rise buildings in the dense urban district using overhang length and glazing type variables with surrogate modelling. *Journal of Physics: Conference Series*. IOP Publishing.
- Ewins, R., 2013. A review of computational optimisation methods applied to sustainable building design. *Renew. Sustain. Energy Rev.* 22, 230–245.
- Fathy, F., Sabry, H., Faggal, A.A., 2017. External Versus Internal Solar Screen: Simulation Analysis for Optimal Daylighting and Energy Savings in an Office Space. In: *Proceedings of the PLEA*, Edinburgh, UK, p. 16.
- Fortich Mora, F.E., 2020. *Humble Giants: Computational Intelligence for Designing More Sustainable High-rise Buildings using Surrogate Models*, <http://resolver.tudelft.nl/uuid:d6d3d3e6-6424-4650-88e2-8d741112257f>.
- Giostra, S., Masera, G., Pesenti, M., Pavesi, P., 2019. Use of 3D tessellation in curtain wall facades to improve visual comfort and energy production in buildings. In: *IOP Conference Series: Earth and Environmental Science*. IOP Publishing, p. 012044.
- Hansen, N., 2006. The CMA evolution strategy: a comparing review. In: *Towards a new evolutionary computation*. Springer, pp. 75–102.
- Hansen, N., Müller, S.D., Koumoutsakos, P., 2003. Reducing the time complexity of the derandomized evolution strategy with covariance matrix adaptation (CMA-ES). *Evol. Comput.* 11 (1), 1–18.
- Hansen, N., Ostermeier, A., 2001. Completely derandomized self-adaptation in evolution strategies. *Evol. Comput.* 9 (2), 159–195.
- IES, 2013. *Approved method: IES spatial Daylight autonomy (sDA) and annual sunlight exposure (ASE)*.
- Ilunga, G., Leitão, A., 2018. Derivative-free Methods for Structural Optimization. In: *Proceedings of the 36th eCAADe Conference*, Lodz, Poland, pp. 19–21.
- Jia, D., Zheng, G., Qu, B., Khan, M.K., 2011. A hybrid particle swarm optimization algorithm for high-dimensional problems. *Comput. Ind. Eng.* 61 (4), 1117–1122.
- Kazanasmaz, T., Grobe, L.O., Bauer, C., Krehel, M., Wittkopf, S., 2016. Three approaches to optimize optical properties and size of a South-facing window for spatial Daylight Autonomy. *Build. Environ.* 102, 243–256.
- Mallipeddi, R., Suganthan, P.N., 2010. Ensemble of constraint handling techniques. *IEEE Trans. Evol. Comput.* 14 (4), 561–579.
- Mallipeddi, R., Suganthan, P.N., Pan, Q.-K., Tasgetiren, M.F., 2011. Differential evolution algorithm with ensemble of parameters and mutation strategies. *Appl. Soft Comput.* 11 (2), 1679–1696.
- Mangkuto, R.A., Dewi, D.K., Herwandani, A.A., Koerniawan, M.D., 2019. Design optimisation of internal shading device in multiple scenarios: Case study in Bandung, Indonesia. *J. Build. Eng.* 24, 100745.
- Mangkuto, R.A., Feradi, F., Putra, R.E., Atmodipoeo, R.T., Favero, F., 2018. Optimisation of daylight admission based on modifications of light shelf design parameters. *J. Build. Eng.* 18, 195–209.
- Oldfield, P., Trabucco, D., Wood, A., 2009. Five energy generations of tall buildings: an historical analysis of energy consumption in high-rise buildings. *J. Arch.* 14 (5), 591–613.
- Palarino, C., Piderit, M.B., 2020. Optimisation of Passive Solar Design Strategies in Side-lit Offices: Maximising Daylight Penetration While Reducing the Risk of Glare in Different Chilean Climate Contexts. *J. Daylight.* 7 (1), 107–121.
- Pilechiha, P., Mahdavinjad, M., Rahimian, F.P., Carnemolla, P., Seyedzadeh, S., 2020. Multi-objective optimisation framework for designing office windows: quality of view, daylight and energy efficiency. *Appl. Energy* 261, 114356.
- Rafiei, M.H., Adeli, H., 2016. Sustainability in highrise building design and construction. *Struct. Des. Tall Spec. Build.* 25 (13), 643–658.
- Rutten, D., 2015. *Grasshopper3D*, <https://www.grasshopper3d.com/>.
- Sherif, A., Sabry, H., Wagdy, A., Mashaly, I., Arafa, R., 2016. Shaping the slats of hospital patient room window blinds for daylighting and external view under desert clear skies. *Sol. Energy* 133, 1–13.
- Smith, A.E., Coit, D.W., 1997. Penalty functions. *Handbook of evolutionary computation* 97(1), C5.
- Storn, R., Price, K., 1997. Differential evolution—a simple and efficient heuristic for global optimization over continuous spaces. *J. Global Optim.* 11 (4), 341–359.
- Tabadkani, A., Banihashemi, S., Hosseini, M.R., 2018. Daylighting and visual comfort of oriental sun responsive skins: A parametric analysis. *Springer* 663–676.
- Touloupaki, E., Theodosiou, T., 2017. Performance simulation integrated in parametric 3D modeling as a method for early stage design optimization—A review. *Energies* 10 (5), 637.
- Vera, S., Uribe, D., Bustamante, W., Molina, G., 2017. Optimization of a fixed exterior complex fenestration system considering visual comfort and energy performance criteria. *Build. Environ.* 113, 163–174.
- Wagdy, A., Elghazi, Y., Abdalwahab, S., Hassan, A., 2015. The balance between daylighting and thermal performance based on exploiting the kaleidocycle typology in hot arid climate of Aswan. *Egypt. AEI* 2015, 300–315.
- Wagdy, A., Sherif, A., Sabry, H., Arafa, R., Mashaly, I., 2017. Daylighting simulation for the configuration of external sun-breakers on south oriented windows of hospital patient rooms under a clear desert sky. *Sol. Energy* 149, 164–175.
- Waibel, C., Wortmann, T., Evins, R., Carmeliet, J., 2019. Building energy optimization: An extensive benchmark of global search algorithms. *Energy Build.* 187, 218–240.
- Wolpert, D.H., Macready, W.G., 1997. No free lunch theorems for optimization. *IEEE Trans. Evol. Comput.* 1 (1), 67–82.
- Wood, A., 2007. Sustainability: a new high-rise vernacular? *The structural design of tall and special buildings* 16(4), 401–410.
- Wortmann, T., 2017a. Model-based optimization for architectural design: Optimizing daylight and glare in grasshopper. *Technology| Architecture+ Design* 1 (2), 176–185.
- Wortmann, T., 2017. *Opossum-introducing and evaluating a model-based optimization tool for grasshopper*.
- Wortmann, T., Natanian, J., 2020. Multi-Objective Optimization for Zero-Energy Urban Design in China: A Benchmark. In: *Proc. SimAUD2020*, pp. 203–210.
- Yi, Y.K., 2019. Building facade multi-objective optimization for daylight and aesthetical perception. *Build. Environ.* 156, 178–190.
- Yi, Y.K., Sharston, R., Barakat, D., 2018. Auxetic structures and advanced daylight control systems. *J. Facade Des. Eng.* 7 (1), 63–74.
- Zargar, S.H., Alaghmandan, M., 2019. CORAL: introducing a fully computational plug-in for stadium design and optimization; a case study of finding optimal spectators' viewing angle. *Arch. Sci. Rev.* 62 (2), 160–170.
- Zhang, R., Waibel, C., Wortmann, T., 2020. Aerodynamic Shape Optimization for High-Rise Conceptual Design: Integrating and validating parametric design, (fast) fluid dynamics, structural analysis and optimization, Anthropologic-Architecture and Fabrication in the cognitive age. In: *Proceedings of the 38th International Online Conference on Education and Research in Computer Aided Architectural Design in Europe*, Berlin, Germany, 16th–17th September 2020. eCAADe (Education and Research in Computer Aided Architectural Design in Europe), pp. 37–45.